Published in final edited form as:
Mol Cancer Ther. 2010 June ; 9(6): 1638–1646. doi:10.1158/1535-7163.MCT-10-0097.

GLOBAL TARGETING OF SUBCELLULAR Hsp90 NETWORKS FOR THERAPY OF GLIOBLASTOMA*

Markus D. Siegelin[1], **Janet Plescia**[1], **Christopher M. Raskett**[1], **Candace A. Gilbert**[2], **Alonzo H. Ross**[2], and **Dario C. Altieri**[1]

[1] Department of Cancer Biology, University of Massachusetts Medical School, Worcester, MA 01605

[2] Department of Biochemistry and Molecular Pharmacology, University of Massachusetts Medical School, Worcester, MA 01605

Abstract

Drug discovery for complex and heterogeneous tumors now aims at dismantling global networks of disease maintenance, but the subcellular requirements of this approach are not understood. Here, we simultaneously targeted the multiple subcellular compartments of the molecular chaperone Heat Shock Protein-90 (Hsp90) in a model of glioblastoma, a highly lethal human malignancy in urgent need of fresh therapeutic strategies. Treatment of cultured or patient-derived glioblastoma cells with Shepherdin, a dual peptidomimetic inhibitor of mitochondrial and cytosolic Hsp90, caused irreversible collapse of mitochondria, degradation of Hsp90 client proteins in the cytosol, and tumor cell killing by apoptosis and autophagy. Stereotactic or systemic delivery of Shepherdin was well tolerated, and suppressed intracranial glioma growth via inhibition of cell proliferation, induction of apoptosis and reduction of angiogenesis, in vivo. These data demonstrate that disabling Hsp90 cancer networks in their multiple subcellular compartments improves strategies for drug discovery, and may provide novel molecular therapy for highly recalcitrant human tumors.

Keywords

Glioma; Shepherdin; Hsp90; apoptosis; autophagy; mitochondria

INTRODUCTION

Despite a better understanding of cancer genes (1), the survival rates of many human tumors have only marginally improved over several decades. This likely reflects the extraordinary molecular and genetic heterogeneity of the transformed cell (2), which, combined with the multilayer redundancy of cancer signaling pathways (3), promotes cellular adaptation and multidrug resistance (4). These challenges are exemplified by glioblastomas, a group of heterogeneous and highly malignant primary brain tumors with survival rates that rarely exceed 12 to 15 months after diagnosis (5). Although progress has been made in uncovering core pathways often deregulated in glioblastoma (6), this has not translated in better therapeutic options in the clinic (7–9), pressing the need for fresh approaches in the management of these patients (10).

Correspondence: Dario C. Altieri, M.D., Department of Cancer Biology, LRB428, 364 Plantation Street, Worcester, MA 01605, Tel. (508) 856-5775; FAX (508) 856-5792; dario.altieri@umassmed.edu.

Conflict of Interest: The authors declare that no conflict of interest exists.

Especially for such recalcitrant malignancies, drug discovery platforms are now evolving beyond traditional, single-gene targeting, to simultaneously disable multiple signaling circuitries of disease maintenance (11). An ideal candidate for such "network-oriented" drug discovery is the molecular chaperone Heat Shock Protein-90 (Hsp90) (12), whose ATPase-directed protein folding orchestrates multiple intersecting pathways of cellular adaptation, survival and drug resistance (13). Accordingly, several small molecule Hsp90 inhibitors have been developed, and are currently undergoing clinical testing (14). However, it has become increasingly clear that Hsp90 homeostasis is not arranged randomly in cells, but is spatially organized in multiple, semi-autonomous subcellular compartments. In this context, Hsp90 and Hsp90-like chaperones oversee transcriptional responses in the nucleus (15), control client protein stability and maturation in the cytosol (16), maintain secretory pathways at the endoplasmic reticulum (17), and preserve mitochondrial integrity, especially in tumors (18), by suppressing cyclophilin D (CypD)-dependent permeability transition (19). Whether this subcellular compartmentalization of the chaperoning network is important for Hsp90-based therapy is currently unknown. However, it is intriguing that none of the structurally diverse Hsp90 inhibitors developed so far has the ability to accumulate in mitochondria (20), suggesting that current therapeutic strategies do not encompass the globality of Hsp90 homeostasis, and this may affect their anticancer efficacy in the clinic(14).

In this study, we asked whether *global* targeting of Hsp90 homeostasis in its multiple subcellular compartments, including mitochondria (18), could better fulfill the concept of "network inhibition" in controlling complex and traditionally recalcitrant tumors, i.e. glioblastoma. We found that a cell- and mitochondrial-permeable peptidomimetic inhibitor of Hsp90 ATPase activity, Shepherdin (18,21), induced collapse of mitochondria and loss of Hsp90 client proteins in the cytosol, providing strong, single-agent anti-glioma activity in vivo, without systemic or organ toxicity.

MATERIALS AND METHODS

Patient samples

Twelve surgically resected samples of WHO grade IV glioblastomas containing adjacent normal brain were collected, and analyzed anonymously as discarded tissue by immunohistochemistry. The patient population comprised both males and females 27 to 79 years of age.

Cells and cell cultures

Human glioblastoma cell lines LN229 (mutant p53, wild type PTEN), U87 (wild-type p53, mutant PTEN), U251 (mutant p53), or normal fetal human astrocytes (FHAS) were purchased from the American Type Culture Collection (ATCC, Manassas, VA), or ScienCell Research Laboratories (Carlsbad, CA). Patient-derived, primary cultures of glioblastoma cells (GS620, GS48 and AS515) were established mycoplasma-free from surgically resected WHO grades IV and III glioblastomas. The glial origin of these cultures was confirmed by staining for α-glial fibrillary acidic protein (Dako), whereas antibodies against endothelial cell markers, CD31 (PharMingen) or factor VIII (Dako), or neuronal neurofilament proteins 70, 160, and 200 (all from Progen), were unreactive.

Antibodies

Antibodies to LC3, Beclin-1 (1:1000, CST Inc., Danvers, MA), Cyclophilin-D (CypD), COX-IV (1:1000, Calbiochem), cytochrome-c (1:1000 Clontech, USA), Hsp70 (1:1000, Abcam, Cambridge, MA), Bcl-2 (1:1000, CST. Inc., Danvers, MA), survivin (1:1000, NOVUS Biologicals, Littleton, CO), XIAP (1:1000 BD, Franklin Lakes, NJ), Ser 473-phosphorylated Akt (1:500, CST. Inc., Danvers, MA), and Akt (1:1000, CST. Inc., Danvers, MA) were used.

Peptidomimetics

The cell- and mitochondrial-permeable peptidomimetic Hsp90 inhibitor, Shepherdin was characterized previously (18,21), and synthesized in the reverse orientation employing all D-amino acids as follows: free/biotin-X-KKWKMRRNQFWVKVQRLFACGSSHK-$CONH_2$ (a cell-permeable *Antennapedia* helix III sequence is underlined; X, hexanoic acid spacer). A cell-permeable scrambled peptidomimetic was also synthesized with D-amino acids in the reverse orientation as follows: free/biotin-X-KKWKMRRNQFWVKVQRGHSFCALKS-$CONH_2$, and used as control (18,21). All peptidomimetics were dissolved in water and buffered to pH 7.4.

Apoptosis and autophagy

The various cell types were seeded in triplicates onto 96-well plates at 2×10^3 cells/well, treated with Shepherdin or scrambled peptidomimetic (0–100 μM) for up to 24 h, and analyzed for metabolic activity by an MTT assay, as described (21). For determination of apoptosis, control or Shepherdin-treated glioblastoma cells (1×10^6) were labeled for Annexin V plus propidium iodide (PI) (BD Bioscience, USA), or, alternatively, for DEVDase (Asp-Glu-Val-Asp, caspase) activity/PI (CaspaTag, Intergen, Burlington, MA), by multiparametric flow cytometry (Becton Dickinson, USA), as described (18,21). To quantify changes in mitochondrial membrane potential, glioblastoma cells were labeled for 10 min in the dark with the mitochondrial membrane potential–sensitive fluorescent dye, JC-1 (10 μg/ml, Molecular Probes), washed, and analyzed for modulation of red/green (FL-2/FL-1) fluorescence ratio, by flow cytometry (18). In some experiments, glioblastoma cells were transfected with non-targeting or CypD-directed SMARTPool siRNA (Dharmacon) (18), using Oligofectamine 2000, confirmed for protein knockdown by Western blotting, and analyzed for cell viability by MTT or mitochondrial membrane potential. For characterization of autophagy, glioblastoma cells were transfected with an LC3-GFP cDNA by LipofectAmine, treated with Shepherdin or scrambled peptidomimetic, and analyzed by fluorescence microscopy. A cell was scored as autophagic when exhibiting a punctate GFP labeling with >10 LC3-GFP dots/cell. An average of 200 cells was counted in 4–6 independent fields per condition.

Preclinical glioblastoma models

All experiments involving animals were approved by an Institutional Animal Care and Use Committee. U87 glioblastoma cells stably transfected with a luciferase expression plasmid (U87-Luc) were suspended in sterile PBS, pH 7.2, and stereotactically implanted (1×10^5) in the right cerebral striatum of immunocompromised CB17 SCID/beige female mice (Charles River Laboratories). Animals with established tumors were randomized in two groups (n=10; 5 animals per group), and started on d 8 after implantation on sterile vehicle (PBS, pH 7.2), or Shepherdin (50 mg/kg as daily i.p. injections) for 17 consecutive d. Tumor growth was assessed weekly after i.p injection of 58 mg/kg D-luciferin by bioluminescence imaging using a Xenogen In Vivo Imaging System. In some experiments animals were harvested on day 21 and subjected to histological analysis. In other experiments, mice (n=6; 3 animals per group) carrying established intracranial U87 gliomas were stereotactically injected with a single dose (0.5 mg) of vehicle or Shepherdin at d 8. On d 20, all animals were sacrificed and brain samples were harvested for histologic analysis.

Histology

Patient-derived tissue specimens were stained with hematoxylin-eosin (H&E), or with an antibody to the mitochondrial Hsp90 chaperone, TRAP-1 (BD Biosciences, San Jose, CA), as described (18). Immunoreactive cells were scored semiquantitatively for staining intensity as 0, negative; 1, low; 2, medium; 3, high; and percentage of TRAP-1 expression in the cell population as 0, no expression; 1, <1%; 2, 1–9%; 3, 10–50% and 4, >50%, as described (22).

Brain samples from the various animal groups were stained with H&E or with antibodies to Ki-67 (Zymed) or CD31 (Becton Dicksinson), as described (20). For in situ determination of apoptosis, brain sections were analyzed for terminal deoxynucleotidyl transferase-mediated dUTP nick end labeling (TUNEL, Roche). Images were collected on an Olympus microscope with on-line charge-coupled device camera. Microvessel density in CD31-stained sections was determined using an image analysis algorithm (S. CO LifeScience Co., Garching, Germany), as described (23). In some experiments, cryosections of glioblastoma xenografts treated with vehicle or Shepherdin were stained with a 1:1000 dilution of streptavidin-Texas red (Amersham Biosciences, Buckinghamshire, UK), and intratumoral accumulation of Shepherdin was visualized by fluorescence microscopy.

Statistical analysis

Data were analyzed by two-sided unpaired t-tests using a GraphPad software package (Prism 4.0) for Windows. A p value of 0.05 was considered as statistically significant. Values are expressed as means of triplicate or duplicate experiments. For preclinical studies, the mean and SEM were calculated with mice as the data units.

RESULTS

Selective expression of mitochondrial chaperone TRAP-1 in human gliomas

We began this study by examining a potential differential expression of one of the cytoprotective mitochondrial Hsp90 chaperones, TRAP-1 (18), in human gliomas. Immunohistochemical analysis of human grade IV glioblastomas revealed that TRAP-1 was highly expressed in the tumor cell population (Fig. 1*A*, *B*). Adjacent normal astrocytes did not contain TRAP-1 (Fig. 1*A*, *B*), whereas a low level of TRAP-1 expression was detected in neurons (not shown). TRAP-1 staining under these conditions appeared as a punctate, perinuclear reactivity, with strong to moderate signal intensity in the various glioblastoma cases examined, whereas a control, non-binding IgG was negative (Fig. 1*A*). Consistent with these results, TRAP-1 was abundantly expressed in a panel of human glioblastoma cell lines, but barely detectable in normal human fetal astrocytes (Fig. 1*C*).

Shepherdin induces mitochondrial dysfunction

Treatment of glioblastoma cells with Shepherdin, a cell- and mitochondrial-permeable inhibitor of Hsp90 ATPase activity (18,21), triggered sudden loss of mitochondrial membrane potential (Fig. 2*A*), and discharge of cytochrome c in the cytosol (Fig. 2*B*), two hallmarks of mitochondrial permeability transition (19). In addition, Shepherdin-treated glioblastoma cells exhibited biochemical markers of autophagy, with decreased expression of the autophagy-associated gene, Beclin-1, and appearance of a lipidated, faster migrating form of the ubiquitin-like protein, LC3 (Fig. 2*C*), which is involved in autophagosome formation (24). This was associated with a punctate pattern of LC3-GFP labeling (Fig. 2*D*), characteristic of autophagy (24), in Shepherdin-treated cells. In contrast, a cell-permeable scrambled peptidomimetic did not affect mitochondrial membrane potential (Fig. 2*A*), or cytochrome c release (Fig. 2*B*), and did not induce markers of autophagy in glioblastoma cells (Fig. 2*D*).

Mechanism of Shepherdin mitochondriotoxic activity

To determine the mechanism of mitochondrial dysfunction induced by Shepherdin (19), we next acutely ablated CypD, a pro-apoptotic component of the permeability pore, in glioblastoma cell types. Transfection of LN229 cells with CypD-directed siRNA efficiently silenced the expression of endogenous CypD, whereas a control, non-targeting siRNA was ineffective (Fig. 3*A*). Under these conditions, CypD knockdown partially reversed Shepherdin-induced loss of mitochondrial membrane potential (Fig. 3*B*), and significantly reduced

Shepherdin-mediated glioblastoma cell killing (Fig. 3*C*). In contrast, a non-targeting siRNA (Fig. 3*A*) had no effect on mitochondrial membrane potential (Fig. 3*B*), or tumor cell killing by Shepherdin (Fig. 3*C*).

Multimodal anti-glioma activity of Shepherdin

Consistent with irreversible mitochondrial damage under these conditions, treatment of glioblastoma cell lines (Fig. 4*A*), or patient-derived glioblastoma cultures (Fig. 4*B*) with Shepherdin caused rapid (~3 h), concentration-dependent, and complete loss of metabolic activity, irrespective of p53 or PTEN status. In contrast, Shepherdin did not affect normal human fetal astrocytes (Fig. 4*A*), and a control, scrambled peptidomimetic was ineffective on normal or glioblastoma cell types (Fig. 4*A*, *B*). Shepherdin-mediated tumor cell killing under these conditions had the hallmarks of apoptosis, with extensive cellular labeling for Annexin V (Fig. 4*C*, *top*), and prominent DEVDase, i.e. caspase, activity (Fig. 4*C*, *bottom*), by multiparametric flow cytometry.

In parallel experiments, Shepherdin treatment inhibited Hsp90 chaperone function in the cytosol of glioblastoma cells, resulting in concentration-dependent degradation of multiple cytoprotective Hsp90 client proteins, including Akt and Ser473-phosphorylated Akt, IAP proteins, XIAP and survivin, and Bcl-2 (Fig. 4*D*). In contrast, low-dose Shepherdin did not affect the cellular levels of Hsp70 whereas higher concentrations led to a weak reduction of Hsp70 levels that did not achieve statistical significance (Fig. 4*D*). In control experiments, a scrambled peptidomimetic had no effect on Annexin V labeling, expression of DEVDase activity (Fig. 4*A*), or cytosolic levels of Hsp90 client proteins (Fig. 4*B*) in glioblastoma cells.

Shepherdin suppresses glioma growth, in vivo

Stereotactic implantation of U87-Luc glioblastoma cells in the right cerebral striatum of immunocompromised SCID/beige mice gave rise to exponentially growing tumors, by bioluminescence imaging (Fig. 5*A*). Systemic administration of Shepherdin to these mice suppressed intracranial glioma growth, in vivo (Fig. 5*A*), and significantly prolonged animal survival, even after treatment suspension, as compared with the vehicle group (Fig. 5*B*). Brain specimens of treated animals revealed extensive intraglioma accumulation of Shepherdin, by fluorescence imaging, in vivo, whereas samples from control mice were unreactive (Fig. 5*C*). Systemic treatment with Shepherdin was not associated with systemic or organ toxicity, and did not result in animal weight loss throughout treatment (Fig. 5*D*). In contrast, animals in the vehicle group exhibited progressive weight loss due to advanced disease (Fig. 5*D*). Histologically, intracranial gliomas growing in vehicle-treated mice exhibited an elevated mitotic index, negligible apoptosis, and extensive angiogenesis (Fig. 6*A*, *B*). In contrast, brain sections collected from Shepherdin-treated mice revealed significant inhibition of glioblastoma cell proliferation, increased apoptosis, and suppression of angiogenesis, in vivo (Fig. 6*A*, *B*).

Normal brain, i.e. neurons contains low, but detectable levels of endogenous Hsp90s in mitochondria (this study), and we next asked whether delivery of Shepherdin directly into the brain still provided anti-glioma activity without toxicity. In these experiments, a single stereotactic administration of Shepherdin was sufficient to suppress intracranial glioma growth in implanted SCID/beige mice, whereas animals in the control group exhibited exponential intracranial glioma growth (Supplemental Fig. 1*A*). Histological examination of brain samples collected from Shepherdin-treated mice was unremarkable compared to control animals receiving vehicle (Supplemental Fig. 1*B*). Conversely, stereotactic delivery of Shepherdin significantly inhibited glioblastoma cell proliferation, in vivo (Supplemental Fig. 1*B*, *C*).

DISCUSSION

In this study, we have shown that *global* subcellular targeting of the Hsp90 networks in cytosol and mitochondria with Shepherdin (18,21) provides strong, single-agent activity in preclinical models of glioblastoma, one of the most recalcitrant human malignancies (5). Mechanistically, Shepherdin induced simultaneous collapse of mitochondrial integrity and degradation of multiple Hsp90 client proteins in the cytosol, triggering tumor cell killing by apoptosis and autophagy, without affecting normal astrocytes. When given systemically or stereotactically to mice, Shepherdin-based therapy was remarkably well tolerated at a preclinically-effective dosage of 50 mg/kg/daily, comparable to the therapeutic range of other conventional or targeted anticancer agents, and potently inhibited intracranial glioma growth via induction of apoptosis, suppression of tumor cell proliferation, and reduction of angiogenesis, in vivo.

Although Hsp90-based therapy (12,14) has been intensely pursued as a paradigm of "network-oriented" drug discovery (11), the clinical results with these agents have so far been inferior to the expectations, producing only small gains in cancer patients, and often at a cost of significant toxicities (14). Although several factors may contribute to these results, it is possible that the inability of current Hsp90 inhibitors to target the multiple subcellular pools of the chaperone, especially a cytoprotective fraction in mitochondria that antagonizes CypD-initiated permeability transition (20), may reduce their clinical efficacy. In this context, Shepherdin provides a conceptually and structurally unique Hsp90 ATPase inhibitor, capable of accumulating in both cytosol (21) and mitochondria (18), and thus suited to globally inhibit chaperone homeostasis in its multiple subcellular fractions (13).

Consistent with these predictions, Shepherdin induced sudden and complete collapse of mitochondrial integrity, triggering CypD-dependent permeability transition, and massive induction of apoptosis in glioblastoma cells. Mechanistically, the "mitochondriotropic" properties of Shepherdin depend on its NH_2-terminus *Antennapedia* helix III cell-penetrating sequence (18). Although it is unclear how this region promotes transfer of cargos across biological membranes, including mitochondria (25), *Antennapedia*-conjugated Shepherdin has been shown to readily distribute throughout all submitochondrial compartments in tumor cells, and to physically associate with Hsp90 chaperones inside the organelle (18). In addition to triggering apoptosis, mitochondrial dysfunction has been linked to induction of autophagy (26), and, accordingly, Shepherdin-treated glioblastoma cells exhibited biochemical markers of autophagy, including loss of Beclin-1 and post-translational processing of the LC3 ubiquitin ligase. Although the implications of autophagy for tumor progression are still being elucidated, this process may be important as a cell death mechanism in glioblastoma (24), efficiently activated in response to stress stimuli (27).

The second phenotype induced by Shepherdin involved acute inhibition of Hsp90 chaperoning in the cytosol (12,13), with concomitant loss of multiple cytoprotective client proteins, including Bcl-2, XIAP, survivin, and Akt. In addition to lowering a cellular anti-apoptotic threshold, thus further aiding in anti-glioma activity, this response may contribute to the anti-angiogenic activity of Shepherdin observed here. Accordingly, critical angiogenesis regulators, including HIF-1α (28), and Erk (29), are recognized client proteins of Hsp90, and their acute downregulation after chaperone inhibition may contribute to impaired blood vessel formation. Alternatively, it is possible that angiogenic stimulation may recruit Hsp90s to mitochondria of proliferating, but not quiescent endothelial cells, thus making them susceptible to Shepherdin-induced killing. Conversely, one important difference with non-subcellularly targeted Hsp90 inhibitors is that Shepherdin treatment did not increase the levels of Hsp70 in glioblastoma cells (12). Although the basis for this response remains to be elucidated, the lack of Hsp70 modulation under these conditions may be therapeutically beneficial, as induction of this

chaperone by conventional Hsp90 inhibitors has been linked to suppression of apoptosis and reduced anticancer activity (30).

The strategy of comprehensive subcellular targeting of Hsp90 networks proposed here may offer tangible advantages over current Hsp90 antagonists. One of the most studied agents in this class, the benzoquinone ansamycin derivative 17-allylamino demethoxygeldanamycin (17-AAG) (12,14) has shown modest single-agent activity in glioblastoma models (22,31), often further attenuated by resistance mechanisms (32). Instead, because of its *direct*, "mitochondriotoxic" mechanism of action, Shepherdin kills indistinguishably apoptosis-sensitive or -resistant glioblastoma cell types, irrespective of survival mechanisms, i.e. expression of Bcl-2, that typically reduce the efficacy of apoptosis-based therapeutics, including 17-AAG (33). Second, Shepherdin exerts its anti-glioma activity independently of p53, and regardless of PTEN status, thus providing broader therapeutic prospects for genetically heterogeneous tumors. Third, Shepherdin-based therapy is remarkably well tolerated, in vivo. This likely reflects the differential distribution of Hsp90s in mitochondria of tumors, including glioblastoma (this study), but not most normal tissues (18). Intriguingly, despite the fact that normal neurons are among the few tissues that contain low levels of Hsp90s in mitochondria (18), stereotactical injection of Shepherdin was well tolerated, and exerted potent anti-glioma activity without detectable local or systemic toxicity, in vivo. This suggests that the lower affinity with which Hsp90 in normal tissues binds ATPase directed antagonists (34), including Shepherdin (21), may further contribute to the overall safety of this agent, in vivo.

In summary, these data establish the rationale for the pursuit and development of a novel class of *global* Hsp90 inhibitors (18), including Shepherdin, capable of simultaneously disabling the multiple, subcellularly compartmentalized pools of the chaperone. Such approach may more adequately fulfill the concept of "network-oriented" drug discovery, and offer fresh therapeutic approaches for the management of heterogeneous and otherwise recalcitrant human tumors, including glioblastoma.

Supplementary Material

Refer to Web version on PubMed Central for supplementary material.

Acknowledgments

Financial Support: This work was supported by NIH grants CA78810, CA90917 and CA118005 (DCA), and Deutsche Forschungsgemeinschaft grant, Si 1546/1-1 (MDS).

We thank Drs. Eric Baehrecke and Claire-Marie Sauvageot for reagents, and Kathryn Chase and Neil Aronin for providing the stereotactical frames.

References

1. Vogelstein B, Kinzler KW. Cancer genes and the pathways they control. Nat Med 2004;10:789–99. [PubMed: 15286780]
2. Wood LD, Parsons DW, Jones S, et al. The genomic landscapes of human breast and colorectal cancers. Science 2007;318:1108–13. [PubMed: 17932254]
3. Luo J, Solimini NL, Elledge SJ. Principles of cancer therapy: oncogene and non-oncogene addiction. Cell 2009;136:823–37. [PubMed: 19269363]
4. Stein WD, Bates SE, Fojo T. Intractable cancers: the many faces of multidrug resistance and the many targets it presents for therapeutic attack. Curr Drug Targets 2004;5:333–46. [PubMed: 15134216]
5. Purow B, Schiff D. Advances in the genetics of glioblastoma: are we reaching critical mass? Nat Rev Neurol 2009;5:419–26. [PubMed: 19597514]

6. Comprehensive genomic characterization defines human glioblastoma genes and core pathways. Nature 2008;455:1061–8. [PubMed: 18772890]
7. Brown PD, Krishnan S, Sarkaria JN, et al. Phase I/II trial of erlotinib and temozolomide with radiation therapy in the treatment of newly diagnosed glioblastoma multiforme: North Central Cancer Treatment Group Study N0177. J Clin Oncol 2008;26:5603–9. [PubMed: 18955445]
8. Reardon DA, Desjardins A, Vredenburgh JJ, et al. Phase 2 trial of erlotinib plus sirolimus in adults with recurrent glioblastoma. J Neurooncol 2009;96:219–30. [PubMed: 19562254]
9. Thiessen B, Stewart C, Tsao M, et al. A phase I/II trial of GW572016 (lapatinib) in recurrent glioblastoma multiforme: clinical outcomes, pharmacokinetics and molecular correlation. Cancer Chemother Pharmacol. 2009
10. Lino M, Merlo A. Translating biology into clinic: the case of glioblastoma. Curr Opin Cell Biol 2009;21:311–6. [PubMed: 19217766]
11. Butcher EC. Can cell systems biology rescue drug discovery? Nat Rev Drug Discov 2005;4:461–7. [PubMed: 15915152]
12. Isaacs JS, Xu W, Neckers L. Heat shock protein 90 as a molecular target for cancer therapeutics. Cancer Cell 2003;3:213–7. [PubMed: 12676580]
13. Whitesell L, Lindquist SL. HSP90 and the chaperoning of cancer. Nat Rev Cancer 2005;5:761–72. [PubMed: 16175177]
14. Drysdale MJ, Brough PA, Massey A, Jensen MR, Schoepfer J. Targeting Hsp90 for the treatment of cancer. Curr Opin Drug Discov Devel 2006;9:483–95.
15. Freeman BC, Yamamoto KR. Disassembly of transcriptional regulatory complexes by molecular chaperones. Science 2002;296:2232–5. [PubMed: 12077419]
16. Hartl FU, Hayer-Hartl M. Molecular chaperones in the cytosol: from nascent chain to folded protein. Science 2002;295:1852–8. [PubMed: 11884745]
17. Frey S, Leskovar A, Reinstein J, Buchner J. The ATPase cycle of the endoplasmic chaperone Grp94. J Biol Chem 2007;282:35612–20. [PubMed: 17925398]
18. Kang BH, Plescia J, Dohi T, Rosa J, Doxsey SJ, Altieri DC. Regulation of tumor cell mitochondrial homeostasis by an organelle-specific Hsp90 chaperone network. Cell 2007;131:257–70. [PubMed: 17956728]
19. Green DR, Kroemer G. The pathophysiology of mitochondrial cell death. Science 2004;305:626–9. [PubMed: 15286356]
20. Kang BH, Plescia J, Song HY, et al. Combinatorial drug design targeting multiple cancer signaling networks controlled by mitochondrial Hsp90. J Clin Invest 2009;119:454–64. [PubMed: 19229106]
21. Plescia J, Salz W, Xia F, et al. Rational design of shepherdin, a novel anticancer agent. Cancer Cell 2005;7:457–68. [PubMed: 15894266]
22. Siegelin MD, Habel A, Gaiser T. 17-AAG sensitized malignant glioma cells to death-receptor mediated apoptosis. Neurobiol Dis 2009;33:243–9. [PubMed: 19027068]
23. Gaiser T, Becker MR, Meyer J, Habel A, Siegelin MD. p53-mediated inhibition of angiogenesis in diffuse low-grade astrocytomas. Neurochem Int 2009;54:458–63. [PubMed: 19428789]
24. Jiang H, White EJ, Conrad C, Gomez-Manzano C, Fueyo J. Autophagy pathways in glioblastoma. Methods Enzymol 2009;453:273–86. [PubMed: 19216911]
25. Torchilin VP. Recent approaches to intracellular delivery of drugs and DNA and organelle targeting. Annu Rev Biomed Eng 2006;8:343–75. [PubMed: 16834560]
26. Samudio I, Kurinna S, Ruvolo P, et al. Inhibition of mitochondrial metabolism by methyl-2-cyano-3,12-dioxooleana-1,9-diene-28-oate induces apoptotic or autophagic cell death in chronic myeloid leukemia cells. Mol Cancer Ther 2008;7:1130–9. [PubMed: 18483301]
27. Kanzawa T, Germano IM, Komata T, Ito H, Kondo Y, Kondo S. Role of autophagy in temozolomide-induced cytotoxicity for malignant glioma cells. Cell Death Differ 2004;11:448–57. [PubMed: 14713959]
28. Kim W-Y, Oh SH, Woo J-K, Hong WK, Lee H-Y. Targeting Heat Shock Protein 90 Overrides the Resistance of Lung Cancer Cells by Blocking Radiation-Induced Stabilization of Hypoxia-Inducible Factor-1{alpha}. Cancer Res 2009;69:1624–32. [PubMed: 19176399]

29. Okawa Y, Hideshima T, Steed P, et al. SNX-2112, a selective Hsp90 inhibitor, potently inhibits tumor cell growth, angiogenesis, and osteoclastogenesis in multiple myeloma and other hematologic tumors by abrogating signaling via Akt and ERK. Blood 2009;113:846–55. [PubMed: 18948577]

30. Beere HM. "The stress of dying": the role of heat shock proteins in the regulation of apoptosis. J Cell Sci 2004;117:2641–51. [PubMed: 15169835]

31. Dungey FA, Caldecott KW, Chalmers AJ. Enhanced radiosensitization of human glioma cells by combining inhibition of poly(ADP-ribose) polymerase with inhibition of heat shock protein 90. Mol Cancer Ther 2009;8:2243–54. [PubMed: 19671736]

32. Gaspar N, Sharp SY, Pacey S, et al. Acquired Resistance to 17-Allylamino-17-Demethoxygeldanamycin (17-AAG, Tanespimycin) in Glioblastoma Cells. Cancer Res 2009;69:1966–75. [PubMed: 19244114]

33. Tagscherer KE, Fassl A, Campos B, et al. Apoptosis-based treatment of glioblastomas with ABT-737, a novel small molecule inhibitor of Bcl-2 family proteins. Oncogene 2008;27:6646–56. [PubMed: 18663354]

34. Kamal A, Thao L, Sensintaffar J, et al. A high-affinity conformation of Hsp90 confers tumour selectivity on Hsp90 inhibitors. Nature 2003;425:407–10. [PubMed: 14508491]

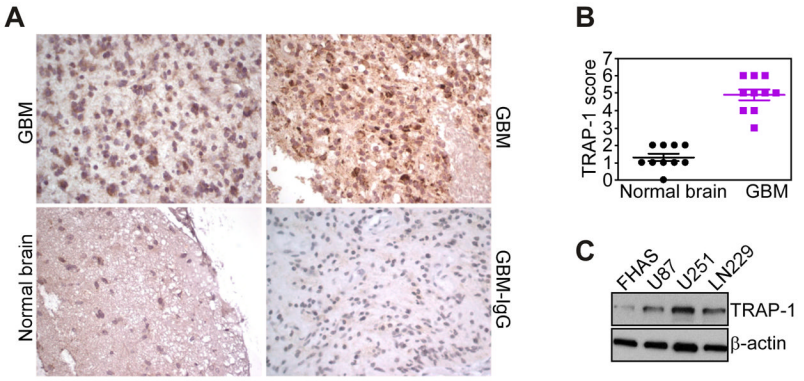

Figure 1.

Differential expression of TRAP-1 in human gliomas. *A*, representative cases of human glioblastoma (GBM), or adjacent normal brain were stained with an antibody to TRAP-1 or IgG (GBM-IgG), and analyzed by immunohistochemistry. Magnification, x100, x200. *B*, quantification of TRAP-1 expression. The indicated samples of glioblastoma (GBM) or adjacent normal brain were scored for TRAP-1 staining intensity and percentage of positive cells. *C*, extracts from U87, U251 or LN229 glioblastoma cells or normal fetal human astrocytes (FHAS) were analyzed by Western blotting.

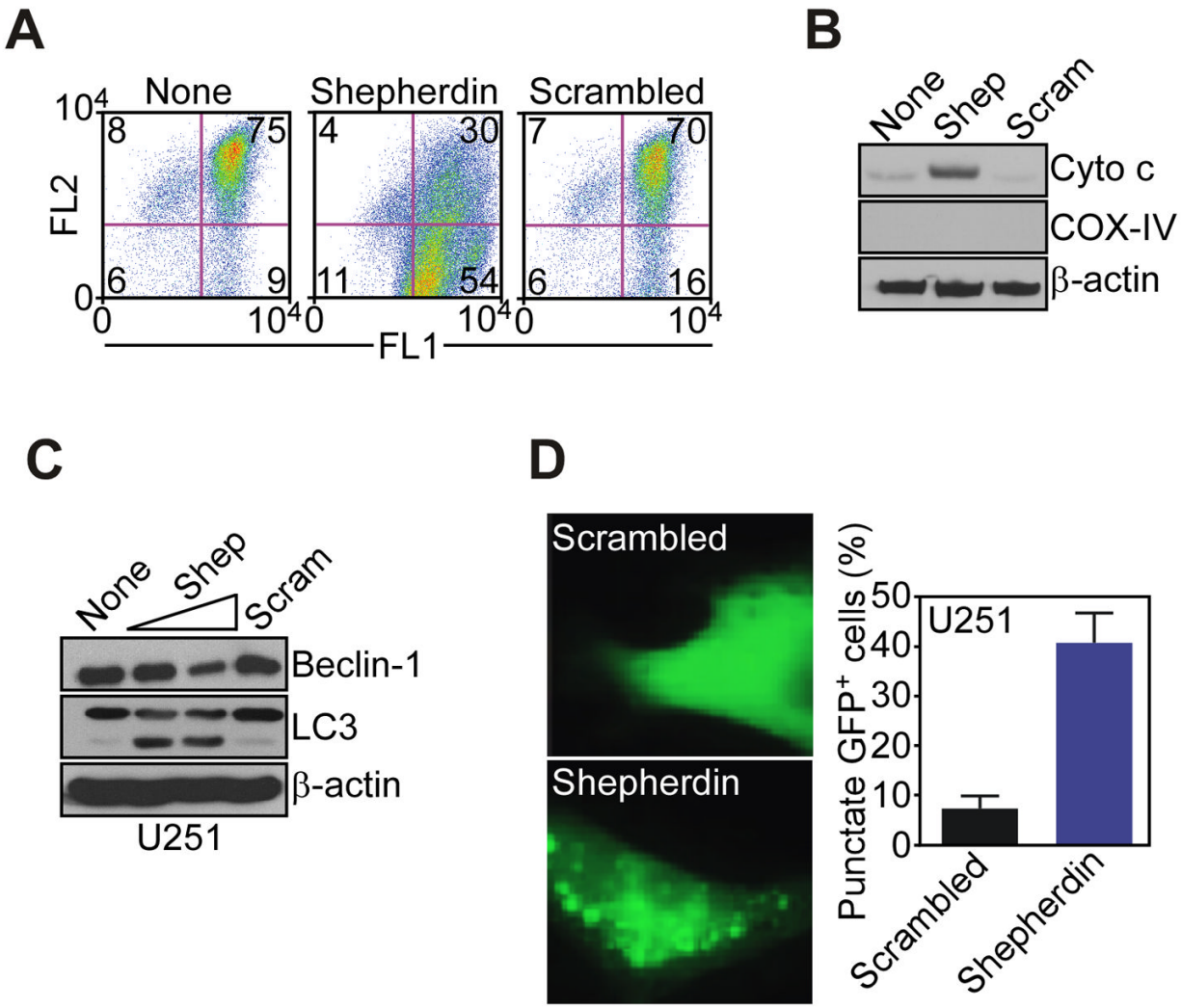

Figure 2.

Shepherdin-induced mitochondrial dysfunction and autophagy. *A*, glioblastoma LN229 cells were incubated with Shepherdin or scrambled peptidomimetic and analyzed for mitochondrial membrane potential by multi-parametric flow-cytometry after 3 h. The percentage of cells in each quadrant is indicated. FL1, green fluorescence channel; FL2: red fluorescence channel. *B*, LN229 cells incubated with Shepherdin (Shep) or scrambled peptidomimetic (Scram) were analyzed by Western blotting after 3 h. *C*, glioblastoma U251 cells treated with Shepherdin (Shep, 50–100 μM) or scrambled peptidomimetic (Scram, 100 μM) were analyzed by Western blotting. *D*, U251 cells transfected with LC3-GFP cDNA were treated with Shepherdin or scrambled peptidomimetic, and analyzed by fluorescence microscopy. *Right*, quantification of cells with punctate GFP staining.

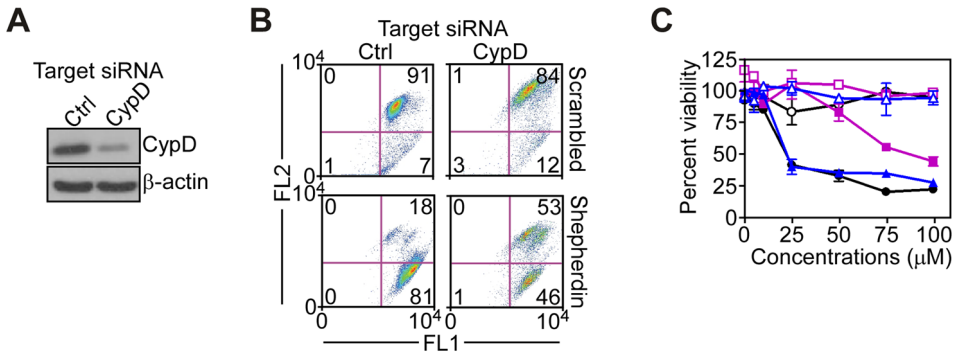

Figure 3.

Requirement of CypD in Shepherdin-induced mitochondrial dysfunction. *A*, LN229 cells were transfected with control, non-targeting or CypD-directed siRNA, and analyzed by Western blotting. *B*, LN229 cells transfected with the indicated siRNA were analyzed for changes in mitochondrial membrane potential after 3 h. The percentage of cells in each quadrant is indicated. FL1, green fluorescence channel; FL2, red fluorescence channel. *C*, LN229 cells transfected with non-targeting (*blue*) or CypD (*purple*)-directed siRNA were left untreated (*black*) or incubated with Shepherdin (*solid symbols*) or scrambled peptidomimetic (*open symbols*), and analyzed by MTT. Data are the mean±SEM.

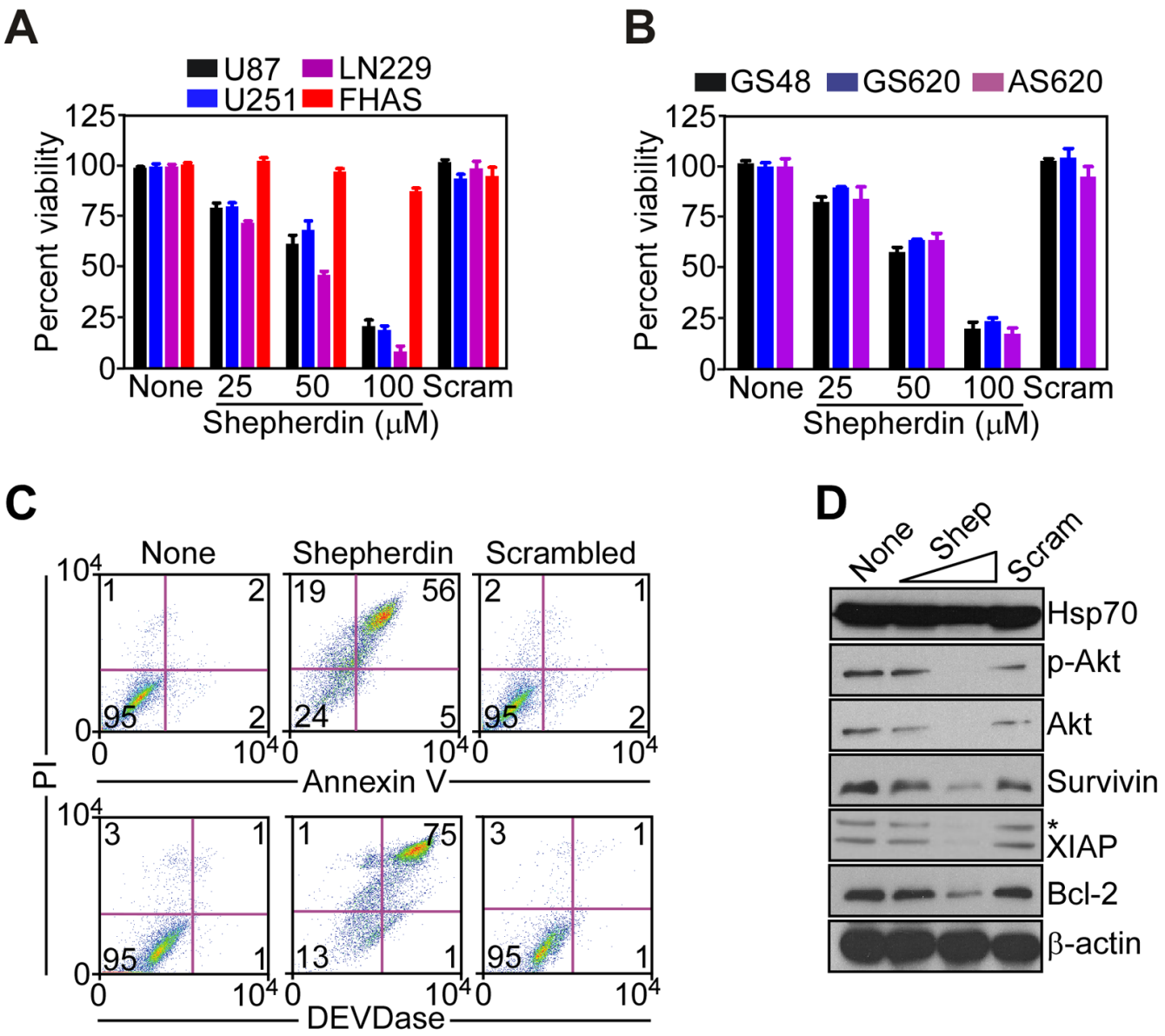

Figure 4.

Multimodal antiglioma activity of Shepherdin. *A*, *B*, The indicated glioblastoma cell lines or FHAS (A), or patient-derived, primary glioblastoma cultures (*B*), were left untreated (None) or incubated with increasing concentrations of Shepherdin or scrambled peptidomimetic (Scram), and analyzed by MTT after 3 h. Data are the mean±SEM, n=3. *C*, untreated (None) or Shepherdin- or scrambled peptidomimetic-treated U87 cells were analyzed after 16 h for Annexin V/PI staining (*top*), or DEVDase (caspase)/PI activity (*bottom*), by multiparametric flow cytometry. The percentage of cells in each quadrant is indicated. *D*, U87 cells treated with Shepherdin (Shep, 50–100 μM) or scrambled peptidomimetic (Scram, 100 μM) were analyzed by Western blotting. p-Akt, Ser473-phosphorylated Akt. *, non-specific.

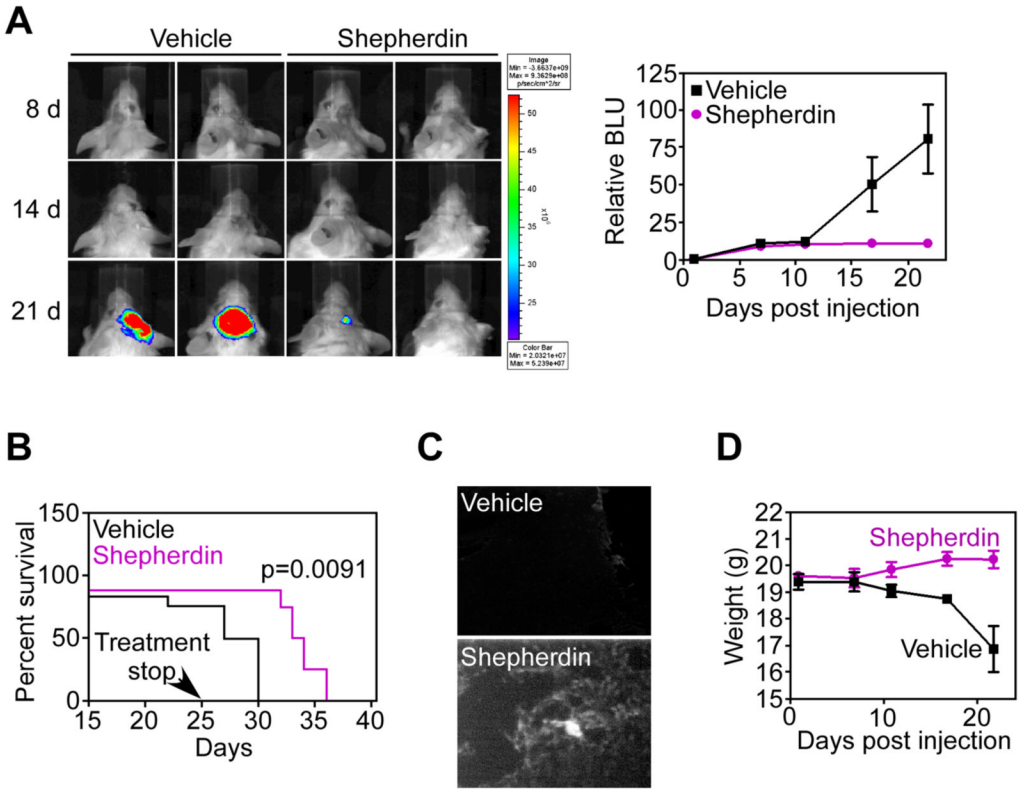

Figure 5.

Anti-glioma activity of Shepherdin, in vivo. *A*, SCID/beige mice stereotactically implanted with U87-Luc cells in the right cerebral striatum were treated systemically with vehicle or Shepherdin (50 mg/kg daily i.p.), and imaged by live bioluminescence at the indicated time intervals. Representative animals per group are shown. *Right*, quantification of bioluminescence units (BLU) in vehicle or Shepherdin-treated groups. Data are the mean±SD of the various groups (5 animals/group). *B*, survival of SCID/beige mice implanted with U87-Luc cells and treated systemically with vehicle or Shepherdin (50 mg/kg daily i.p.). *C*, SCID/beige mice implanted with U87-Luc cells were injected with biotin-conjugated Shepherdin or vehicle, and brain samples were analyzed for intracranial accumulation of Shepherdin by fluorescence microscopy after 24 h. *D*, weight changes in vehicle- or Shepherdin-treated mice. Data are the mean±SD of the various groups (5 animals/group).

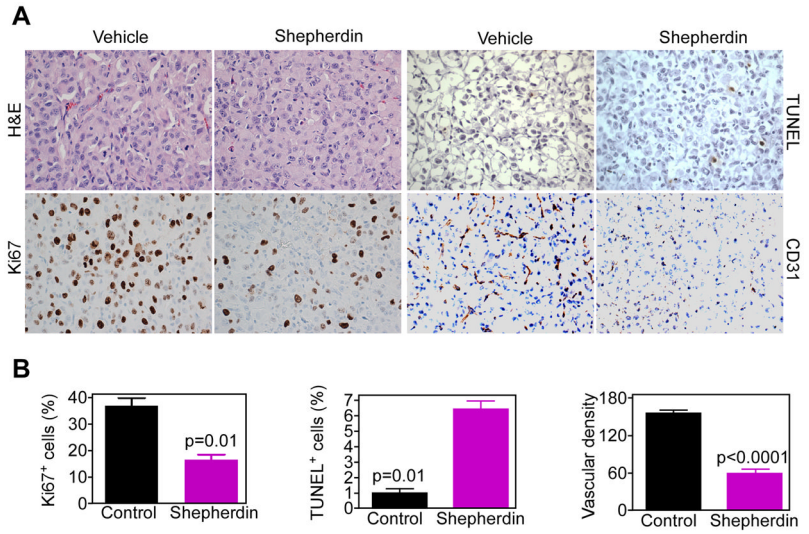

Figure 6.

Histopathology of Shepherdin anti-glioma activity, in vivo. *A*, representative brain sections from vehicle- or Shepherdin-treated mice were harvested after 20 d, and analyzed by H&E, cell proliferation (Ki67), apoptosis (TUNEL), or angiogenesis (CD31), by immunohistochemistry. Magnification, x400. *B*, quantification of mitotic index (*left*), apoptosis (*middle*) and microvessel density (*right*). Labeled cells were counted in an average of 4–6 high- power fields. Data are mean±SEM.